HYDROLOGICAL PROCESSES
Hydrol. Process. **26**, 2592–2600 (2012)
Published online 24 May 2012 in Wiley Online Library
(wileyonlinelibrary.com) DOI: 10.1002/hyp.9325

The effect of peatland harvesting on snow accumulation, ablation and snow surface energy balance

Scott J. Ketcheson,* Peter N. Whittington and Jonathan S. Price

Department of Geography and Environmental Management, University of Waterloo, Waterloo, Ontario, Canada

Abstract:

Snow distribution, ablation and snowmelt energy balance components were characterized in a vacuum harvested and an adjacent undisturbed forested section of a peatland during the 2009 snowmelt period to determine snow distribution and melt dynamics on a previously harvested peatland, since abandoned and partly revegetated. The forested peatland had the deepest snowpack at 121 cm, particularly along the edge of the forested section adjacent to the more windblown previously harvested peatland. The snowpack density was greatest in the harvested peatland, which was subject to greater wind compaction and mid-winter melt-refreeze episodes; however, snow water equivalence was higher in the forested peatland. Radiative fluxes dominated the snowmelt energy balance. Increased canopy cover within the forested peatland restricted incident radiation and delayed melt, whereas melt rates were rapid across the harvested peatland, driven by higher radiant and turbulent fluxes. Ablation calculated using a simple, one-dimensional model showed good temporal agreement with the observed ablation trends except when standing melt water pooled on the surface of the harvested section, causing more rapid modelled melt rates than observed. The shallower snowpack and more rapid melt across the harvested peatland limited the amount of melt water that was available for spring recharge. Copyright © 2012 John Wiley & Sons, Ltd.

KEY WORDS peatland; snowmelt; energy balance; peat harvesting; restoration

Received 26 August 2011; Accepted 30 March 2012

INTRODUCTION

Runoff during the snowmelt period represents a dominant component of the annual water budget in both undisturbed boreal peatlands (Stein *et al*., 1994; Metcalfe and Buttle, 2001) and disturbed systems (Shantz and Price, 2006; Price and Ketcheson, 2009). Globally, peat harvesting is widespread in parts of Scandinavia, Russia, British Isles and North America (Price and Ketcheson, 2009). Although global productivity in natural peatland ecosystems far exceeds the volume of peat harvested annually (Price *et al*., 2003), hydrological and ecological functions at the regional and local scale are profoundly impacted. Peatland harvesting begins with the installation of drainage ditches and the removal of the shrub and tree vegetation cover, which reduces the surface roughness and increases the incoming shortwave radiation incident upon the surface, potentially altering patterns of snow accumulation and the rate of snow melt. Thus, changes in the timing and magnitude of snowmelt runoff may be one of the most pronounced hydrological responses to peatland disturbances. Although few studies have characterized the effect of peatland disturbance on the distribution of snow and, hence, the storage of winter precipitation, less is known about the implications for snowmelt dynamics and the impact on water retention within disturbed peatlands. In most cases, the largest challenge during peatland restoration is the limited water availability (Price *et al*., 2003) that constrains the recolonization of *Sphagnum* mosses in bog peatlands, the dominant peat-forming plant (Kuhry and Vitt, 1996). In harvested peatlands, drainage systems often remain moderately functional after final abandonment (Price *et al*., 2003). Water loss from drainage coupled with the poor water storage capacity of the remnant peat magnifies the impact on plant-water supply (Lavoie *et al*., 2005) and emphasizes the importance of the spring snowmelt recharge period; however, this issue has yet to be sufficiently addressed from a peatland restoration perspective.

Since vegetation canopies play a significant role in snow hydrology because of their impact on snow accumulation patterns (Boon, 2011) and the snow ablation energy balance (Boon, 2009), it is important to understand the effect of their removal on water availability in disturbed peatland ecosystems. Although much is known about snow hydrology in healthy and disturbed forests and forest clearings (e.g. Jeffrey, 1970; Pomeroy *et al*., 2002; Boon, 2009; Boon, 2011), snow processes in harvested peatlands have not been well studied. Differences in snow distribution, characteristics and ablation between forests and forest clearings depends both on factors such as type of forest, relief and climate and on the size of clearing under consideration (Gelfan *et al*., 2004). Snow ablation rates in clearings have been found to be approximately three times as large as in adjacent forests, and melt rates decreased with increasing vegetation leaf area index (Pomeroy and Granger, 1997; Faria *et al*., 2000). The influence of the

*Correspondence to: S. J. Ketcheson, Department of Geography and Environmental Management, University of Waterloo, Waterloo, Ontario, N2L 3G1, Canada.
E-mail: sjketche@uwaterloo.ca

forest canopy in the exchange of water vapour, heat and energy at the snow surface is well documented (e.g. Price and Dunne, 1976; Davis *et al*., 1997; Woo and Giesbrecht, 2000; Gelfan *et al*., 2004); however, basic information on snow accumulation and ablation changes caused by removal of the vegetation during peatland harvesting is lacking. Thus, the objective of this study is to quantify the effects of peatland vacuum harvesting on snow distribution and melt dynamics. Specifically, snow characteristics, the components of the snow surface energy balance and snow ablation rates within a harvested and forested section of a peatland are characterized, with an emphasis on the implications for water availability for peatland restoration.

STUDY SITE

The Bic-Saint-Fabien (BSF) peatland is located within the Saint Lawrence Lowlands, approximately 30 km west of Rimouski, Québec, Canada. Mean annual precipitation recorded at the Rimouski meteorological station is 915 mm, 30% of which falls as snow (Environment Canada, 2011). Average daily temperatures are −12 °C and 18 °C in January and July, respectively (Environment Canada, 2011). The site is underlain by a layer of marine clay deposited by the former Goldthwait Sea, which flooded much of the St. Lawrence Lowlands when the land was depressed and water levels rose following the last glaciation (Dionne, 1977). Extensive auger sampling by E. Sararas (personal communication) indicates that the clay layers are spatially continuous beneath the peatland; thus, water exchanges with the regional system are restricted. Approximately 10.6 ha of the 17.4 ha peatland was harvested and subsequently abandoned using the vacuum peat extraction technique (*Harvested section* in Figure 1) during the period of approximately 1946–2000 (unpublished records). This technique involves installing deep (0.7–1.0 m) drainage ditches and cambering the surface to enhance runoff (Price *et al*., 2003), which causes subsidence due to shrinkage, oxidation and compression (Schothorst, 1977; Kennedy and Price, 2005). As such, the harvested section of the BSF peatland is characterized by a well-decomposed and compacted peat substrate, with very limited spontaneous recolonization of *Sphagnum* mosses. Peat thickness varies between 1.6 and 3.5 m. Some vascular vegetation, mostly *Typha*, has established within the ditches throughout the harvested section; however, this comprises a small (~5%) proportion of the site and was assumed to have a limited effect on snow dynamics. A 6.8-ha forested peatland is situated directly to the north of the harvested section (*Forested section* in Figure 1). The forest vegetation is dominated by black spruce (*Picea mariana*), tamarack (*Larix laricina*) and cedar (*Thuja occidentalis*), with a surface cover dominated by *Sphagnum* moss species.

FIELD MEASUREMENTS

Snow surveys were conducted at least every second day along transects through both the harvested and forested sections of BSF for the duration of the 2009 snowmelt period (31 March to 6 May 2009) (Figure 1). Depth

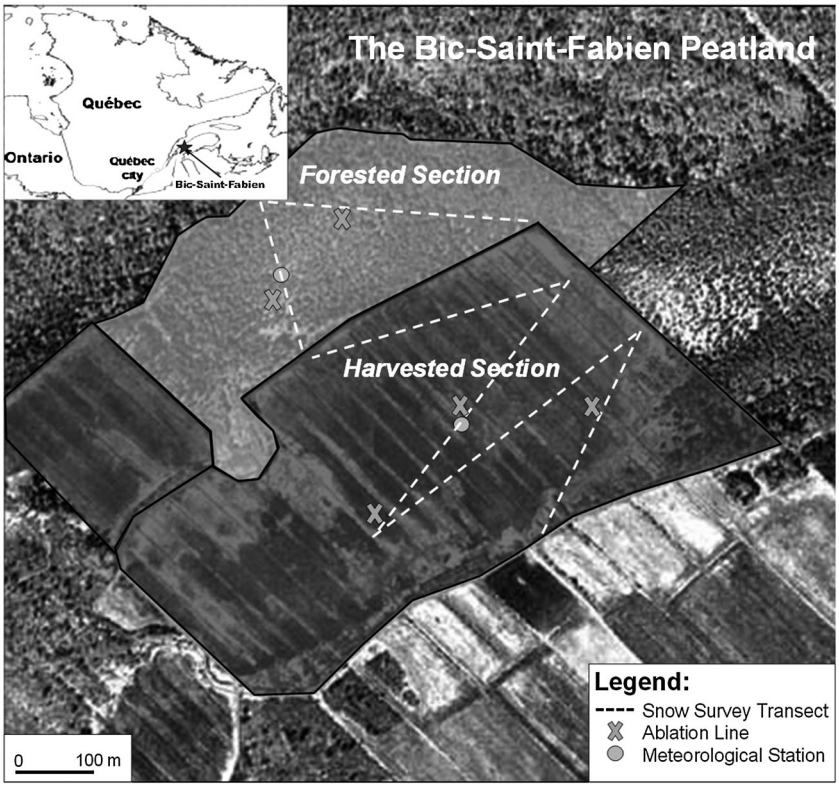

Figure 1. Map of the Bic-Saint-Fabien (BSF) peatland. Snow pits were located at the ablation lines in both sections

measurements were made approximately every 10 m and multiplied by density measurements (collected every 30 m using a standard Meteorological Service of Canada snow sampler) to calculate snow water equivalent (SWE). The sampling protocol was designed such that ditches across the harvested section were sampled in a manner proportional to their occurrence. Wilcoxon rank sum difference of means tests were conducted to determine the statistical significance of observed differences in peak snow depth and SWE measurements (31 March).

Daily ablation was obtained by measuring the lowering of snow surface across several ablation lines (each approximately 7–10 m long) in 50 cm increments and multiplying the surface lowering rate by the average snowpack density (measured with the snow sampler) within each section of the peatland (Woo and Heron, 1987). Snowpack structure and density were measured in a snow pit near each ablation line using standard methods (Adams and Barr, 1974) to identify periods of mid-winter thaw and verify measurements made with the snow sampler.

Meteorological stations were established in both the harvested and forested sections of the BSF peatland. Measurements of air temperature (T_a) and relative humidity (RH) were made every 20 min using Hobo U12 dataloggers (Onset Corporation), while 20-min average values (60-s measurements) of wind speed (μ; O14A Met One Instruments), rainfall (r; Texas Electronics TR-525) and net radiation (Q^*; REBS Q7.1) were recorded using Campbell Scientific dataloggers (see Table I for instrument heights). Because of instrumentation limitations, rainfall measurements were made in a clearing in the forested section and were used to determine r in both the forested and harvested section. Instrumentation constraints did not allow for Q^* to be separated into incoming and outgoing long and shortwave radiation. As such, radiative inputs were represented solely by Q^* measurements.

Snow surface energy balance

The components of the snow ablation energy balance were calculated through a simple, one-dimensional model as

$$Q_m = Q* + H + LE + R + G \quad (1)$$

where Q_m is the total energy available for snow melt, H and LE are fluxes of sensible and latent heat, R is the energy input from rainfall and G is ground heat flux (all units in $W\,m^{-2}$). Because of equipment malfunction preventing *in situ* measurements, G was set to a constant value of $3.13\,W\,m^{-2}$ (USACE, 1956; Maidment, 1993; Boon, 2009), which is a small component of the budget. The evaluation of H and LE typically requires measurement of temperature, wind speed and humidity at two or more levels above the snow surface (Heron and Woo, 1978). However, the lower height can be considered to be that of the snow surface (i.e. $\mu = 0$) (Dingman, 2002), which has a surface humidity of nearly 100% and a temperature of 0 °C during the melt period (Heron and Woo, 1978). The assumption of a logarithmic profile for wind speed and vapour pressure permits the use of the bulk transfer approach to calculate fluxes of sensible and latent heat using wind-speed measurements at only one level (Dingman, 2002). This assumes that there is no radiative or turbulent flux divergence in the surface layer of the atmosphere. Indeed, there will be some deviation from a logarithmic wind profile under conditions of low wind speeds; however, under these conditions turbulent fluxes are suppressed, so inaccuracies in their estimation should not be critical to snowmelt computations (Moore, 1983).

In both sections of BSF, daily H was calculated as a function of the difference between the temperature at the snow surface and the temperature in the overlying air, as

$$H = \rho_a C_{pa} D_H (T_a - T_{ss}) \quad (2)$$

where ρ_a is the density of air ($kg\,m^{-3}$), C_{pa} is the heat capacity of air at constant pressure ($J\,kg^{-1}\,K^{-1}$), D_H is the bulk sensible-heat transfer coefficient ($m\,s^{-1}$) and T_a and T_{ss} are the temperatures of the air and snow surface, respectively (K).

Daily LE was calculated within both sections of BSF as a function of the difference between the vapour pressure at the snow surface and the vapour pressure in the overlying air, as

$$LE = \rho_a \lambda_v D_E \frac{0.622}{P} (e_{a-} e_{ss}) \quad (3)$$

where λ_v is the latent heat of vapourization ($2.48 \times 10^6\,J\,kg^{-1}$), D_E is the bulk latent-heat transfer coefficient ($m\,s^{-1}$), P is the atmospheric pressure (kPa) and e_a and e_{ss} are atmospheric and snow surface vapour pressure (kPa), respectively. Negative LE values indicate energy release from the surface of the snow via evaporation or sublimation, whereas positive LE values represent energy directed into the snowpack as condensation.

Table I. Average daily meteorological variables (± standard deviation) and instrument height for melt period 1 (31 March to 17 April) at Bic-Saint-Fabien

	T_a (°C)	T_a (°C) *max./min.*	Q^* ($W\,m^{-2}$)	μ ($m\,s^{-1}$)	RH (%)	Rainfall (mm)
Harvested	1.4 (±1.4)	6.5 / -1.9	60.0 (±46.5)	2.1 (±1.1)	72.4 (±17.3)	17
Instrument Height	**1.2 m**		**1.3 m**	**1.1 m**	**1.2 m**	
Forested	0.9 (±0.9)	4.5 / -1.9	4.1 (±5.9)	0.2 (±0.1)	77.0 (±15.3)	
Instrument Height	**1.3 m**		**1.4 m**	**1.5 m**	**1.3 m**	

Rainfall represents the total over the same period. T_a *max/min* represents the average daily temperature maximum and minimum values over MP 1.

Under neutral atmospheric conditions, the diffusivities of water vapour and heat are equal (Dingman, 2002). Thus, $D_H = D_E = D$ and

$$D = \frac{k^2 \mu_a}{\left[\ln\left(\frac{z_a}{z_o}\right)\right]^2} \quad (4)$$

where k is von Karman's constant (0.4), μ_a is the wind speed ($m\,s^{-1}$), z_a is the height of the wind measurement (m) and z_o is the surface roughness (m) of the snowpack (Boon, 2009). Field-based measurements of z_o were not possible; however, recent work by Boon (2009) in forested and clear-cut areas used a z_o value of 0.006 m in place of field-based measurements. Given the insensitivity of z_o values within an order of magnitude, this is a reasonable substitution.

The bulk transfer equations are only valid for neutral atmospheric conditions. As such, the Richardson number (Ri) was used to characterize and correct for the stability condition of the atmosphere (Dingman, 2002), where

$$R_i = \frac{g(T_a - T_{ss})}{{\mu_a}^2 T_K} \quad (5)$$

and where g is acceleration due to gravity ($m\,s^{-2}$) and T_K is the mean temperature of the air layer (K). Temperature inversions, common over snow, create stable atmospheric conditions and suppression of turbulence. To correct for the occurrence of stable conditions, identified as $Ri > 0.3$ (Andreas, 2002), D_H and D_E were modified according to Price and Dunne (1976), where

$$D_S = \frac{D}{1 + 10Ri} \quad (6)$$

and where D_S is the drag coefficient under stable conditions ($m\,s^{-1}$). Unstable conditions ($Ri < 0$) are less common (Heron and Woo, 1978) but can be corrected for by

$$D_U = \frac{D}{1 - 10Ri} \quad (7)$$

where D_U is the drag coefficient under unstable conditions ($m\,s^{-1}$). On days when rainfall occurred, R can be evaluated by

$$R = \rho_w c_w r(T_r - T_{ss}) \quad (8)$$

where c_w is the heat capacity of water ($4.19 \times 10^{-3}\,MJ\,kg^{-1}\,K^{-1}$), r is the rainfall rate ($mm\,d^{-1}$) and T_r is the temperature of the rain (K). Because RH is usually close to 100% during rain, it can be assumed that $T_r = T_a$ (Dingman, 2002).

RESULTS

The duration of the snowmelt period in the harvested and forested sections of BSF was 18 and 35 days, respectively. Since the intention of this study is to compare snowmelt dynamics between the harvested and forested sections, it is necessary to address the variables contributing to snowmelt during comparable periods. As such, the forested section results are discussed in terms of both the duration of the harvested melt period (herein referred to as melt period 1 or MP1; 31 March to 17 April), to facilitate a comparison between the two sections, and the duration of the forested section melt period (melt period 2 or MP2; 31 March to 4 May), which includes MP1 and extends 17 days longer until the forested section is deemed to be snow free.

Meteorological variables

Air temperatures followed similar trends in both the forested and harvested sections of BSF during MP1; however, average daily air temperatures in the harvested section were higher than those in the forested section on all but one day (Table I). Rainfall during MP1 totaled 17 mm, and one trace snowfall event was observed, which likely contributed approximately 1 mm water equivalent to the snowpack. During MP2, there was an additional 58 mm of rainfall, most of which occurred as a single rainfall event (43 mm) that lasted 3 days and ended on 23 April. Both the average daily wind speed and net radiation within the forested section was an order of magnitude less than that in the harvested section during MP1, whereas relative humidity was typically higher and less variable within the forest (Table I).

Snow characteristics

Just prior to melt (31 March 2009), median peak snowpack depth was much greater in the forested section (93 cm) than the harvested section (46 cm), with the deepest snowpack along the edge of the forested section (max. depth = 121 cm) (Figure 2). The observed differences between both snow depth and SWE in the harvested and forested sections were statistically significant ($p < 0.0001$) based on Wilcoxon rank sum difference of means tests. Variability in snowpack characteristics was comparable between the forested and harvested sections (Figure 2). In the forested section, this was largely driven by variability in forest canopy cover and tree density, whereas the presence of drainage ditches caused much of the observed variability throughout the harvested section. The median water equivalent of the peak snowpack for the harvested and forested sections was 16 and 27 cm, respectively, despite a slightly greater and more variable snowpack density in the harvested section. Snow pit data indicate that the snowpack density was more uniform with depth in the forested section ($0.33 \pm 0.04\,g\,cm^{-3}$) than the harvested section ($0.43 \pm 0.09\,g\,cm^{-3}$). Also, an approximately 1 cm thick ice layer was present at roughly 20 cm depth within the snowpack at over half of the snow pits across the harvested section, indicative of a short mid-winter melt episode. Conversely, an ice layer in the forested section (~30 cm depth) appeared to be less continuous, as it was encountered at less than 25% of snow pits.

Bi-daily snow surveys throughout the snowmelt period (31 March to 4 May 2009) indicated that the snowpack depleted more rapidly across the harvested section than

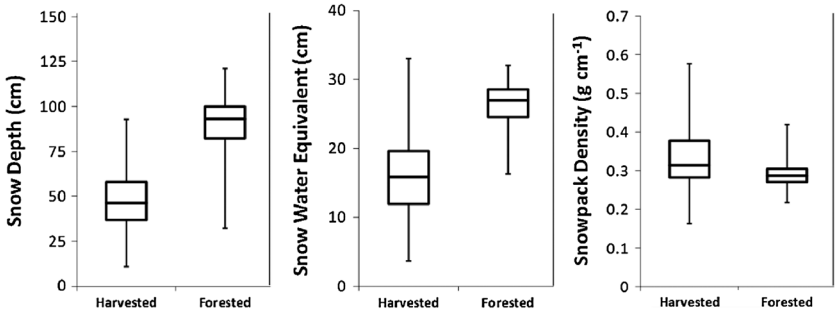

Figure 2. Box plots of peak snow depth, snow water equivalent (SWE) and snowpack density at BSF on 31 March 2009. This highlights snow accumulation differences between the harvested and forested sections of the peatland. Snow depth n = 128 and 62 for the harvested and forested sections, respectively. SWE n = 45 and 24 for the harvested and forested sections, respectively

the forested section (Figure 3A). Snow cover on the harvested section of the site became increasingly patchy soon after the onset of melt, with the emergence of areas with melt water pooled atop the frozen, sometimes snow-covered, cutover peat surface in early April (Figure 3B). Initiated by an exceptionally high average daily air temperature on 3 April (5 and 4 °C for the harvested and forested sections, respectively), half of the snow in the harvested section melted rapidly between 3 and 6 April, resulting in the emergence of both exposed peat (bare surface) and pooled melt water. The average ablation rate in the harvested section during this period was 13 mm SWE day^{-1}, whereas the forested ablation rate was 9 mm SWE day^{-1} (Figure 4). Nearly half of the surface in the harvested section was covered by standing melt water by 6 April (average depth 31 cm), which represented a dominant portion of the surface cover across the harvested section until the majority of the pooled melt water had flowed off of the site by 13 April (Figure 3B). The harvested section became more than 75% snow-free by 17 April, with drifts of snow remaining within the ditches and around the perimeter of the site for slightly longer (snow surveys in the harvested section ceased at this time, so the timing of the ablation of the remnant snow patches was not quantified). In contrast, the forested section still had a relatively uniform snow cover until late April, and deep patches of snow persisted until the section was considered to be snow-free (>75% snow-free) on 4 May (Table II). Ablation line measurements indicated that daily melt rates were higher in the harvested section than the forested section throughout MP1 (Figure 4). Standing water was not observed in the forested section.

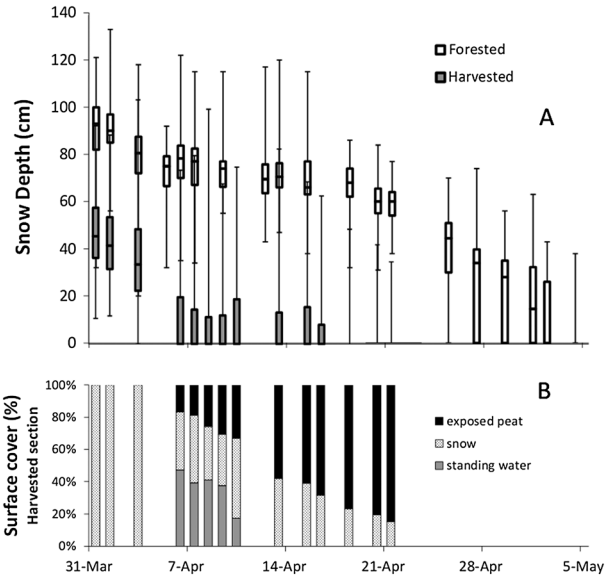

Figure 3. A) Box plots of snow depth for the snowmelt period in 2009. Deeper snowpack and slower ablation rates in the forested section (clear boxes) results in a prolonged persistence of snow cover compared with the harvested section (shaded boxes). Greater spread across the median in the harvested section indicates more variability in snowpack depth compared to the forested section. B) Proportion of the harvested section covered by snow, standing water and exposed peat (bare surface) during the harvested section melt period. Note that standing water within the harvested section was initially mostly water on snow/ice, thereby causing the apparent snow cover to increase once the standing water drained away, as a thin slushy cover was often left behind, which artificially increased the proportion of the site considered to have a snow cover

Snow ablation energy balance

The total energy available for snow melt was positive on the first day of measurement in both the harvested and forested sections, which indicates that the snowpack had likely ripened prior to instrumentation. Greatly reduced wind speeds within the forested section resulted in ablation being largely driven by radiative fluxes, whereas harvested section ablation was driven by a combination of radiation and turbulent fluxes. Net radiation was much lower in the forested section than the harvested section, resulting in greatly reduced energy available for melt (Figures 5 and 6). Large temperature gradients caused by higher air temperatures above the snow surface in the harvested section, along with consistently higher wind speeds, resulted in daily sensible heat fluxes an order of magnitude greater in the harvested section than the forested section (Figure 5). Daily sensible heat fluxes in the harvested section were highest at the beginning of the melt period when warm air temperatures caused large temperature gradients over the snow (Figure 6). Throughout MP1, H in the forested section remained modest, as cooler air temperatures constrained temperature gradients and lower wind speeds further suppressed turbulent heat exchange.

Latent heat flux was predominantly an energy loss from the snow surface (Figure 5), with the exception of the early snowmelt period when atmospheric conditions were

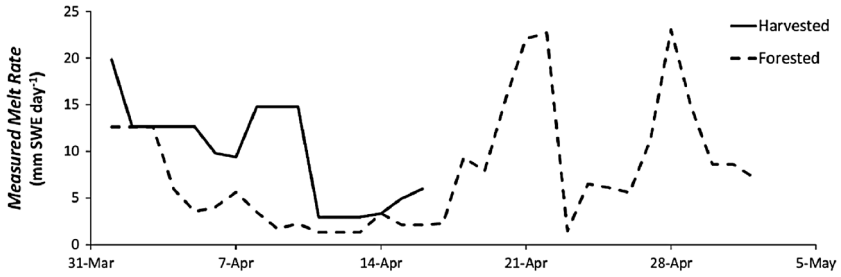

Figure 4. Measured daily melt rates in the harvested and forested sections of BSF

Table II. Average snowpack properties during melt period 1 (harvested section; 31 March to 17 April) and melt period 2 (forested section; 31 March to 4 May), respectively

Section	Average depth (cm)	Density ($g\,cm^{-3}$)	SWE (cm)	Date of snow removal		Duration of melt period (days)*
				50% snow-free	>75% snow-free	
Harvested	23	0.36	13	6 April	17 April	18
Forested	54	0.34	20	1 May	4 May	35

*Time from start of snowmelt period (31 March) until >75% snow-free.

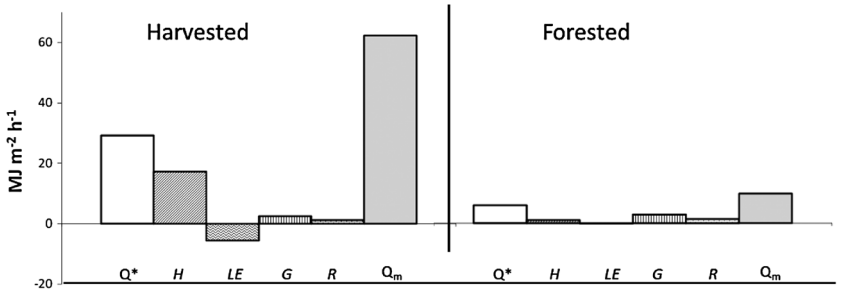

Figure 5. Cumulative energy balance components in the harvested (left) and forested (right) sections of BSF during the harvested melt period (note this only includes the period up until the modelled snow-free date, 31 March to 10 April 2009)

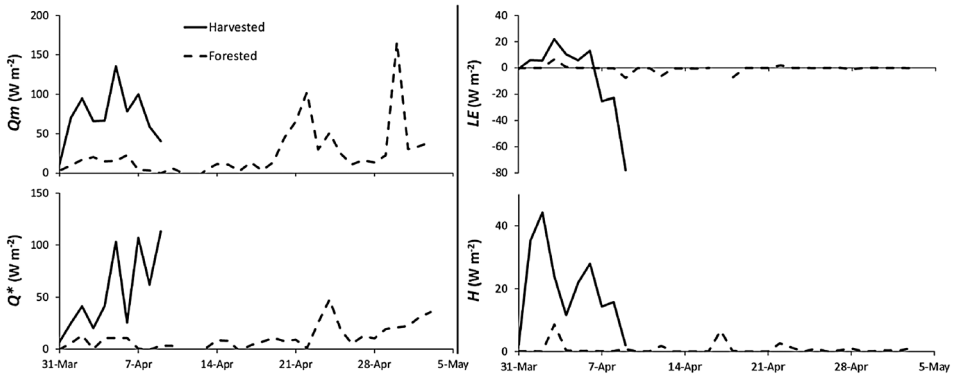

Figure 6. Average daily melt energy and individual energy balance components from one-dimensional model calculations in the harvested and forested sections of BSF in 2009 for the entire melt period (the harvested section line ends at the beginning of the modelled snow-free period on 10 April)

very humid (Figure 6). As with fluxes of sensible heat, daily latent heat fluxes were substantially higher in the harvested section. This was driven by greater wind speeds and larger differences between the vapour pressure at the snow surface and the vapour pressure in the overlying air within the harvested section. R was typically a small fraction of the snow ablation energy balance (Figure 5), accounting for $1.3\,MJ\,m^{-2}\,h^{-1}$ in both sections of BSF, which represented

2% and 13% of the total energy available for melt in the harvested and forested sections, respectively, during MP1. The 43-mm rain event on 21 and 23 April represented the largest contribution of R (> 50% of the MP2 total) to ablation in the forested section and caused the highest modelled and measured ablation rates during the forested section snowmelt period, as reflected in the steep slope of the SWE depletion curves (Figure 7). Average daily air temperature during this event was nearly 4 °C, which contributed to the measured ablation rate of 23 mm SWE day^{-1} (Figure 4). This high ablation rate was nearly matched on 28 April because of an average daily air temperature exceeding 6 °C.

Model performance

In the harvested section, measured and modelled snowmelt showed relatively good agreement until 6 April, which coincided with the emergence of standing melt water that caused an increase in Q* at the meteorological station because of less reflective melt water replacing the high albedo snow cover. Much of the harvested section was covered in snow; however, the net radiometer was centered over an area of standing water and, thus, did not account for the reflection of incident radiation caused by the albedo of the snow. As such, modelled ablation rates, as driven higher by unrepresentatively large Q* values, exceeded measured ablation rates and resulted in the model underestimating the duration of the snowmelt period by 7 days in the harvested section (Figure 7). In the forested section, the modelled daily melt rate was close to the measured rate – except for the first 5 days when the rapid snow depletion was not simulated by the model. This difference may be partly explained by more rapid settling of the snowpack near to the ablation line used for the manual measurements. Nonetheless, the trend of the modelled ablation shows good temporal agreement with the observed ablation trends, indicating good agreement between the calculated Q_m and the actual depletion of the snowpack in the forested section (Figure 7). The measurement period within the forested section ended on 8 May, at which point 95% of the original SWE had been melted by the model, signifying that the model overestimated snowpack removal in the forested section by 5 days.

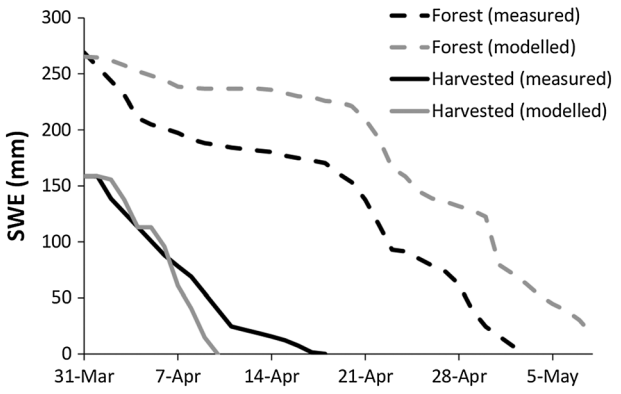

Figure 7. Measured (black line) and modelled (grey line) SWE depletion curves for the harvested (solid line) and forested (dashed line) sections of BSF

DISCUSSION

Snow distribution and melt dynamics

Removal of the vegetation canopy during peat extraction has a profound impact on snow hydrology. Net radiation measured within the forested section was an order of magnitude less than that measured over the harvested section during MP1 (Figure 5; 31 March to 17 April) where the vegetation cover was removed for peat extraction. Since snow ablation is driven largely by radiation, ablation rates measured within the harvested section were often twice those measured in the forested section (Figure 7). Furthermore, the consistently higher wind speeds in the harvested section facilitated fluxes of turbulent energy (H and LE) that were an order of magnitude greater in the open harvested section (Figure 5). Consequently, ablation duration was nearly twice as long in the forested section than the harvested section (Table II). Long-wave radiation emission from the canopy and tree trunks within the forested section will contribute to melting of the snowpack; however, this additional melt energy likely only accounts for a small fraction of the total shortwave radiation that is blocked by the canopy (Metcalfe and Buttle, 1998).

The presence of the vegetation cover in the forested section enhanced deposition and limited the scour of snow that resulted in a deeper peak snowpack and higher SWE in the forested section compared with the harvested section (Figure 2). These results are in opposition to more typical snow relations between cleared sites relative to forested sites. A previous study by Gelfan *et al*. (2004) reported SWE values in an open agricultural catchment that were, on average, 12% greater than those observed in a forested basin over a 17 year observation period. Other studies have demonstrated that the removal of forest vegetation has been associated with a large increase of snow accumulation (Pomeroy *et al*., 1998) and ablation rates (Pomeroy and Granger, 1997). In addition, clear-cut sites typically exhibit greater SWE than nearby forested areas, in part because of the elimination of canopy interception and subsequent sublimation of intercepted snow (Storck *et al*., 1999; Gelfan *et al*., 2004; Buttle *et al*., 2005) and in part because of redistribution of snow to clear-cuts (Murray and Buttle, 2003). As such, clear-cuts often represent a control plot to characterize maximum snow depth and SWE expected in open areas around the landscape (Boon, 2009). However, in clearings with a width greater than 20 times the height of the surrounding trees, the wind speed is relatively unaffected by the trees, and snow accumulation in the clearing may be less than that in the forested area (Murray and Buttle, 2003). For example, Shantz and Price (2006) observed significantly greater ($p = 0.05$) snow depth and SWE within the forested section of a peatland in Eastern Canada as compared with the harvested section of the same peatland. The current study observed lower SWE and a more shallow snow depth within the harvested section at BSF (Figure 2), likely because of the effects of wind on snowpack dynamics and redistribution.

Within the forested section, the vegetation stand reduced the wind speed (Table I), which trapped wind-blown snow and caused accumulation rates to exceed those in the harvested section (Figure 2). Furthermore, the sublimation of wind-blown snow particles can greatly reduce the amount of snowfall that remains on the surface in areas subjected to higher wind speeds (Pomeroy and Essery, 1999; Liston and Sturm, 2002), such as the harvested section at BSF. The harvested section snowpack was also affected by a mid-winter melt episode (see *Snow Characteristics* section) that contributed to the increased density and reduced snow depth throughout the harvested section. The presence of the ice layer within the snowpack (above the underlying ground surface) indicates that the melt event only affected the density (increase) and depth (decrease) and had no impact on the SWE.

Drainage ditches installed during the peat harvesting process (apparent as striations across the harvested section of BSF in Figure 1) caused the increased variability in snowpack characteristics observed in the harvested section (Figure 2), as the ditches extended approximately 0.7 to 1.0 m below the typically flat cutover peat surface and also contained emergent vegetation, which trapped snow. The deeper snow within these ditches skewed the snow depth and, hence, SWE towards higher values. However, as indicated in the *Field Measurements* section, the measurements included proportional sampling of ditches.

The forested peatland canopy absorbed and reflected incoming shortwave radiation, which strongly constrained the amount of energy available for melt at the snow surface (Figure 5). Furthermore, because the upward rate of turbulent heat transport depends on the product of the wind speed and the difference between the vapour pressure (for *LE*) or temperature (for *H*) at the surface and the vapour pressure (or temperature) in the overlying air (Dingman, 2002), reduced wind speeds suppressed turbulent heat transfers in the forested section (Figures 5 and 6). Thus, Q_m was constrained further, which consequently reduced ablation rates in the forested section as compared with those in the harvested section, as reflected in the more gradual slope of the measured and modelled SWE depletion curves (Figure 7).

Timing of snowmelt and implications for restoration

Changes in snow surface energy input to the harvested section caused by peat extraction strongly impacted snow distribution and the rate of melt. The daily melt rate in the harvested section consistently exceeded that of the forested section (Figures 4 and 7), often by as much as two times, whereas the SWE in the harvested section was just over half that of the forested section (Table II). The smaller amount of snow on the harvested section, coupled with the increased melt rate, consequently decreases both the duration of the melt period and the amount of water available from the snow cover. Furthermore, frost depth has been shown to increase when the depth of the snowpack is reduced (Groffman *et al.*, 2001; Groffman *et al.*, 2006); thus, the cutover peat substrate in the harvested section likely has deeper ground frost caused by the observed reduced snowpack depth. Thus, the surface remains frozen and essentially impermeable during the spring recharge period, which allows very little water to recharge the peat water storage deficit. Moreover, the rapidity of melt, low microtopography of harvested sites and frozen ground resulted in surface flooding and rapid runoff and water loss through the semi-functional drainage ditches. Blocking drainage ditches or construction of bunds to retain snowmelt water are sometimes used in restoration attempts (e.g. Shantz and Price, 2006; Ketcheson and Price, 2011), but no attempts have been made to increase snow accumulation with snow retention structures such as snow fences or targeted vegetation species with desired snow retention characteristics. This would, to an extent, reduce the depth of ground frost and would facilitate the retention of increased amounts of winter snowfall on harvested sites. Although Q_m would remain more or less unaffected, the increased amount of snow accumulation over the winter season would prolong the snowmelt period and result in more water available for spring recharge. With a thinner frozen soil layer, higher peak SWE and slightly prolonged melt period, conditions would be more favourable for increased retention of spring snowmelt waters.

CONCLUSION

Since wind speed influence on snow distribution and ablation is driven largely by incoming shortwave radiation, removal of the vegetation cover during peat extraction has a substantial impact on snow hydrology and a strong influence on snow accumulation and ablation processes. Wind speeds were low in the forested section of the peatland, resulting in increased deposition and limited scour of snow by wind and, thus, a deeper peak snowpack and higher SWE. Lower wind speeds in the forested section also constrained the amount of snowmelt caused by turbulent heat transfer by inhibiting steep temperature and humidity gradients near the snow surface. Consequently, melt rates in the harvested section were often twice those observed in the forested section, and the snowmelt period was 17 days shorter. Removal of the vegetation from peatlands during peat extraction has substantial impacts on snow accumulation and ablation processes. Rapid and early melt in harvested peatlands constrains the amount of water retained on site, a requisite for restoration.

ACKNOWLEDGEMENTS

We would like to thank Colin McCarter and Evan Price for their work in the field. This work was funded by the National Science and Engineering Research Council through the Industrial Research Chair (Rochefort) and Discovery Grant (Price) programs. Thanks as well to Vicky Bérubé for providing aerial imagery and to Murray Richardson for assistance with statistical analysis. The comments of two anonymous reviewers helped to improve this manuscript.

REFERENCES

Adams W, Barr D. 1974. Techniques and equipment for measurement of snow cover, including stratigraphy. *Measurement in Physical Geography: Trent University, occasional papers* **3**: 11–26.

Andreas EL. 2002. Parameterizing scalar transfer over snow and ice: a review. *Journal of Hydrometeorology* **3**: 417–432.

Boon S. 2009. Snow ablation energy balance in a dead forest stand. *Hydrological Processes* **23**: 2600–2610.

Boon S. 2011. Snow accumulation following forest disturbance. *Ecohydrology* **2011**. DOI: 10.1002/eco.212

ButtleJM, Oswald CJ, Woods DT. 2005. Hydrologic recovery of snow accumulation and melt following harvesting in northeastern Ontario. *Proceedings of the Eastern Snow Conference* **62**: 83–91.

Davis R, Hardy JP, Ni W, Woodcock J, McKenzie JC, Jordan R, Li X. 1997. Variation of snow cover ablation in the boreal forest: A sensitivity study on the effects of conifer canopy. *Journal of Geophysical Research D. Atmospheres* **102**: 29389–29395.

Dingman SL. 2002. *Physical Hydrology Second Edition*. Prentice Hall: Upper Saddle River, New Jersey.

Dionne J-C. 1977. La mer de Goldthwait au Québec. *Géographie physique et Quaternaire* **31**: 61–80.

Environment Canada. 2011. Canadian Climate Normals 1971–2000. Environment Canada.

Faria D, Pomeroy J, Essery R. 2000. Effect of covariance between ablation and snow water equivalent on depletion of snow covered area in a forest. *Hydrological Processes* **14**: 2683–2695.

Gelfan A, Pomeroy J, Kuchment L. 2004. Modelling forest cover influences on snow accumulation, sublimation, and melt. *Journal of Hydrometeorology* **5**: 785–803.

Groffman PM, Driscoll CT, Fahey TJ, Hardy JP, Fitzhugh RD, Tierney GL. 2001. Colder soils in a warmer world: a snow manipulation study in a northern hardwood forest ecosystem. *Biogeochemistry* **56**: 135–150.

Groffman PM, Hardy JP, Driscoll CT, Fahey TJ. 2006. Snow depth, soil freezing, and fluxes of carbon dioxide, nitrous oxide and methane in a northern hardwood forest. *Global Change Biology* **12**(9): 1748–1760.

Heron R, Woo M. 1978. Snowmelt computations for a high Arctic site, 35th Eastern Snow Conference, 162–172.

Jeffrey W. 1970. Snow hydrology in the forest environment, Snow hydrology: Proceedings. Workshop seminar on snow hydrology, Fredericton, 28–29 Feb. 1969, 1–19.

Kennedy GW, Price JS. 2005. A conceptual model of volume-change controls on the hydrology of cutover peats. *Journal of Hydrology* **302**: 13–27.

Ketcheson SJ, Price JS. 2011. The impact of peatland restoration on the site hydrology of an abandoned block-cut bog. *Wetlands* **31**: 1263–1274.

Kuhry P, Vitt DH. 1996. Fossil carbon/nitrogen ratios as a measure of peat decomposition. *Ecology* **77**: 271–275.

Lavoie C, Saint-Louis A, Lachance D. 2005. Vegetation dynamics on an abandoned vacuum-mined peatland: 5 years of monitoring. *Wetlands Ecology and Management* **13**: 621–633.

Liston GE, Sturm M. 2002. Winter Precipitation Patterns in Arctic Alaska Determined from a Blowing-Snow Model and Snow-Depth Observations. *Journal of Hydrometeorology* **3**: 646–659.

Maidment D. 1993. *Handbook of Hydrology, 1424*. McGraw Hill Professional: New York.

Metcalfe R, Buttle J. 2001. Soil partitioning and surface store controls on spring runoff from a boreal forest peatland basin in north central Manitoba, Canada. *Hydrological Processes* **15**: 2305–2324.

Metcalfe RA, Buttle JM. 1998. A statistical model of spatially distributed snowmelt rates in a boreal forest basin. *Hydrological Processes* **12**: 1701–1722.

Moore RD. 1983. On the use of bulk aerodynamic formulae. *Nordic Hydrology* **14**: 193–206.

Murray CD, Buttle JM. 2003. Impacts of clearcut harvesting on snow accumulation and melt in a northern hardwood forest. *Journal of Hydrology* **271**: 197–212.

Pomeroy JW, Granger R. 1997. Sustainability of the western Canadian boreal forest under changing hydrological conditions. I. Snow accumulation and ablation. *IAHS Publication* **240**: 237–242.

Pomeroy JW, Gray DM, Shook KR, Toth B, Essery RLH, Pietroniro A, Hedstrom N. 1998. An evaluation of snow accumulation and ablation processes for land surface modelling. *Hydrological Processes* **12**: 2339–2367.

Pomeroy JW, Essery R. 1999. Turbulent fluxes during blowing snow: field tests of model sublimation predictions. *Hydrological Processes* **13**: 2963–2975.

Pomeroy JW, Gray DM, Hedstrom NR, Janowicz JR. 2002. Prediction of seasonal snow accumulation in cold climate forests. *Hydrological Processes* **16**: 3543–3558.

Price A, Dunne T. 1976. Energy balance computations of snowmelt in a subarctic area. *Water Resources Research* **12**: 686–694.

Price JS, Heathwaite AL, Baird AJ. 2003. Hydrological processes in abandoned and restored peatlands: An overview of management approaches. *Wetlands Ecology and Management* **11**: 65–83.

Price JS, Ketcheson SJ. 2009. Water relations in cutover peatlands, Carbon Cycling in Northern Peatlands. Geophys. Monogr. Ser. AGU, Washington, DC, 277–287.

Schothorst CJ. 1977. Subsidence of low moor peat soil in the western Netherlands. *Geoderma* **17**: 265–291.

Shantz M, Price J. 2006. Characterization of surface storage and runoff patterns following peatland restoration, Quebec, Canada. *Hydrological Processes* **20**: 3799–3814.

Stein J, Proulx S, Lévesque D. 1994. Forest floor frost dynamics during spring snowmelt in a boreal forested basin. *Water Resources Research* **30**: 995–1007.

Storck P, Lettenmaier DP, Bolton S. 1999. Measurement of snow interception and canopy effects on snow accumulation and melt in a mountainous maritime climate, Oregon, United States. *Water Resources Research* **38**.

United States Army Corps of Engineers. 1956. *Snow Hydrology: Summary Report of the Snow Investigations*, US Army Corps of Engineers, North Pacific Division: Portland, OR.

Woo M, Giesbrecht M. 2000. Simulation of snowmelt in a subarctic spruce woodland: 1. Tree model. *Water Resources Research* **36**: 2275–2285.

Woo MK, Heron R. 1987. Effects of forests on wetland runoff during spring. *Forest Hydrology and Watershed Management. International Association of Hydrological Sciences* **167**: 297–307.

